www.sciencemag.org/content/354/6314/893/suppl/DC1

Supplementary Materials for

The sacral autonomic outflow is sympathetic

I. Espinosa-Medina, O. Saha, F. Boismoreau, Z. Chettouh,
F. Rossi, W. D. Richardson, J.-F. Brunet*

*Corresponding author. Email: jfbrunet@biologie.ens.fr

Published 18 November 2016, *Science* **354**, 893 (2016)
DOI: 10.1126/science.aah5454

This PDF file includes:

Other Supplementary Material for this manuscript includes the following:
(available at www.sciencemag.org/cgi/content/full/354/6314/893/DC1)

Movies S1 and S2

Materials and Methods

Histology.

-In situ hybridization and immunochemistry have been described in ref *(32)*.

-Diaphorase staining on cryostat sections was performed as described in ref *(33)*.

-Immunofluorescence on cryostat or vibratome sections was performed as previously described *(25)*. Whole-processed embryos where fixed overnight in 4% paraformaldehyde (in PBS) and dissected spinal cords were fixed for 2 hours at room temperature. Antigen retrieval, by boiling for 10 minutes in sodium citrate (10mM) was needed for optimal labeling with the α-Islet antibody.

Wholemount immunofluorescent staining using the 3DISCO method was adapted from ref *(34)*. All steps up to the imaging of the embryos were performed under nutation. Embryos at stage E11.5 were fixed overnight in 4% paraformaldehyde (in PBS), serially dehydrated in graded methanol (in PBS) up to 100% methanol and then bleached using Dent's bleach overnight at 4°C. Following serial washes in 100% methanol, the embryos were incubated in Dent's fixative overnight at 4°C. The embryos were then serially rehydrated in graded methanol (in PBS) up until re-immersion in PBS. Embryos were further subjected to incubation at 70°C to optimize antigen recognition by the anti-Phox2b antibody. Following washes in PBS-Tween (0.1%), tiny superficial perforations were made in the embryo with a minutien pin to facilitate antibody penetration. The embryos were then incubated with primary antibodies in blocking buffer (20% DMSO, 5% FCS in PBS) for 5 days at room temperature. Following washes in PBS-Tween (0.1%) at room temperature, secondary antibodies in blocking buffer were then applied for 4 days at room temperature. Finally, embryos were cleared following the 3DISCO protocol subsequent to washes in PBS-Tween (0.1%) at room temperature, Embryos were imaged using a SP8 confocal microscope (Leica). 3D reconstructions and videos were obtained using the IMARIS imaging software.

Antibodies

The following primary antibodies were used for immunochemistry and immunofluorescent staining:

α-2H3 (NF), Mouse, 1:500, Hybridoma Bank (#2H3)
α-bIII Tubulin (Tuj1), Mouse, 1:500, Covance (#MMS-435P)
α-dsRed, Rabbit, 1:500, Clontech (#632496)
α-Tomato, Goat, 1:1000, Sicgen (#AB0040-200)
α-Islet1:2, Mouse, 1:400 (40.2D6 and 39.4D5, Hybridoma Bank)
α-Phox2b, Rabbit, 1:500 *(35)*
α-Phox2b, Guinea Pig, 1:500 *(36)*
α-Phox2a, Rabbit, 1:500 *(37)*
α-Sox10, Goat, 1:250, Santa Cruz (#SC-17342)
α-FoxP1, Rabbit, Abcam,1:200 (#AB-16645)

The following secondary antibodies were used:

α-rabbit Cy3, 1:500, Jackson Immunoresearch Laboratories (#711-165-152)
α-rabbit A488, 1:500, Jackson Immunoresearch Laboratories (#711-545-152)
α-goat Cy3, 1:500, Jackson Immunoresearch Laboratories (#705-166-147)
α-goat A647, 1:500, Jackson Immunoresearch Laboratories (#705-606-147)
α-rabbit Cy3, 1:500, Jackson Immunoresearch Laboratories (#711-165-152)
α-mouse Cy3, 1:500, Jackson Immunoresearch Laboratories (#715-165-150)
α-mouse A488, 1:500, Invitrogen (#A-21202)
α-mouse Cy5, 1:500, Jackson Immunoresearch Laboratories (#715-175-150)

Immunohistochemical reactions were processed with the Vectastain Elite ABC kits (PK-6101 and PK-6012; Vector Laboratories) as per manufacturer's guidelines followed by colour development using DAB (3,3'-Diaminobenzidine).

Probes

For the Phox2b riboprobe, primers containing SP6 and T7 overhangs were used to amplify a 635 bp region (nucleotides 123 – 757) from a plasmid containing the full-length Phox2b cDNA sequence. The purified amplicon was then used as the template for antisense probe synthesis using T7 RNA polymerase.

Forward Primer: 5'-CCGTCTCCACATCCATCTTT-3'

Reverse Primer: 5'-TCAGTGCTCTTGGCCTCTTT-3'

The other probes were: Gata3 (gift of JD Engel), Hand1 (Stratagene), Hmx2 (gift of E.E. Turner), Hmx3 (gift of S. Mansour), Islet1 *(37)*, Tbx2 (gift of A. Kispert), Tbx3 (gift of V.M Christoffels), Tbx20 *(38)*, VAChT (Source BioScience, UK, 40129421 (CK3-a14) IMAGE clone).

Transgenic Mouse Lines:

-Phox2b::Cre (39): BAC transgenic line expressing Cre under the control of the Phox2b promoter.

-Rosa$^{lox\text{-}stop\text{-}lox\text{-}tdTomato}$ (*Rosa*^{tdT}) *(40)*: Knock in line expressing the reporter gene tdTomato from the Rosa locus in a Cre-dependent manner.

-Phox2b$^{LacZ/+}$ line *(31)*: Knock in line expressing the reporter gene *LacZ* from the second exon of the *Phox2b* locus, which is disrupted and lead to a null phenotype in *Phox2b*$^{LacZ/LacZ}$ embryos.

-Olig2Cre line *(41)*: Knock in of Cre in the *Olig2* locus (Jackson Laboratories, Stock #25567).

All animal studies were done in accordance with the guidelines issued by the French Ministry of Agriculture and have been approved by the Direction Départementale des Services Vétérinaires de Paris.

Image Analyses.

To measure the size of the pelvic ganglion on cryosections from E13.5 *Olig2*$^{+/—}$ and *Olig2*$^{—/—}$ embryos hybridized for Phox2b and immunostained for neurofilament, we used the open source image analyses tool ilastik *(42)*. Pixels were segmented by a Random Forest Classifier into signal (corresponding to the pelvic ganglion) and background (corresponding to surrounding tissues and nerve fibers). Segmentation on one section was

optimized through an iterative training procedure based on color/intensity, edge and texture, and subsequently applied to the batch processing of all sections passing through one pelvic ganglion. Local neighborhoods for calculating edge and texture were defined as 3 X 3 pixels and 5 X 5 pixels. Finally, scattered signal areas smaller than 0.2μm2 were removed on FIJI. The remaining signal area corresponded to the pelvic ganglion and was measured on 5 to 6 consecutive sections, depending on ganglia. The volume of the ganglion was deduced by multiplying the surface by the thickness of the sections (20μm). Wild-type and mutant ganglia were compared by a paired two-tailed Student's t-test.

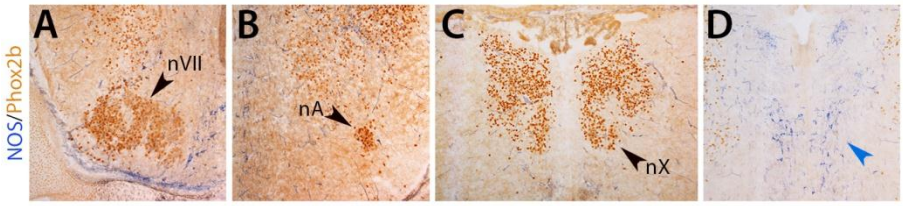

Figure S1

NOS is not expressed neither in branchiomotor neurons nor in hindbrain preganglionic neurons. Transverse sections of the hindbrain at E17.5 stained for diaphorase activity and Phox2b immunohistochemisty and passing through: (A) the facial nucleus (nVII); (B) the nucleus ambiguus (nA); (C) the dorsal nucleus of the vagus nerve (nX); (D) the pons, showing NOS+ neurons of the raphe (blue arrowhead). No double Phox2b+/NOS+ neurons were found in the hindbrain.

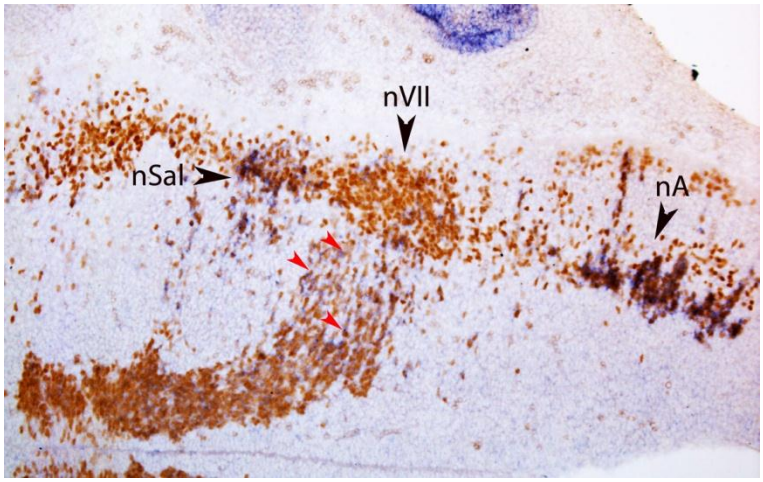

Figure S2

Expression of Tbx3 in all branchial and visceral motoneurons of the hindbrain. Longitudinal section though an E11.5 medulla, stained by combined Phox2b immunohostochemistry and *Tbx3* in situ hybridization. In addition to nX (Fig. 2), *Tbx3* is expressed in salivatory motoneurons (nSal) and the nucleus ambiguus (nA). Expression is also found in a subset of migrating facial motoneuronal precursors (red arrowheads). nVII: facial motor nucleus.

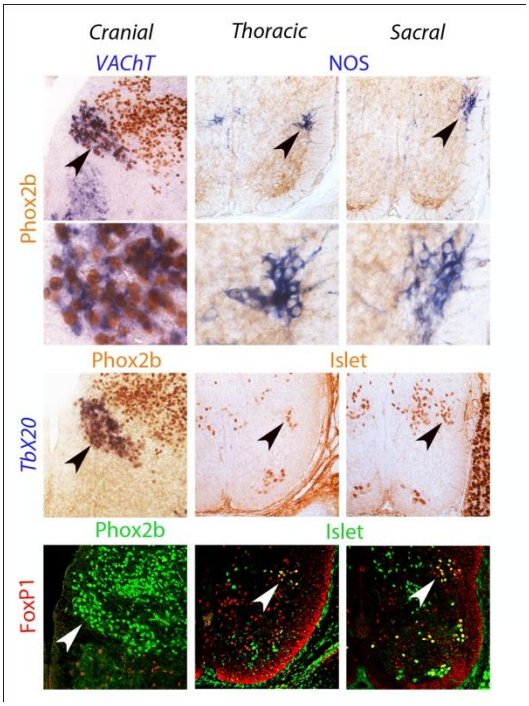

Figure S3

Maintenance at E16.5 of a parasympathetic genetic signature by cranial preganglionics and of a sympathetic genetic signature by both thoracic and sacral preganglionics. Transverse sections at E16.5 through the right half of the medulla (left column), thoracolumbar spinal cord (middle column) and sacral spinal cord (right column), stained with the indicated antibodies and probes. Arrowheads point to the nX in the left column and to spinal preganglionics in the middle and right columns.

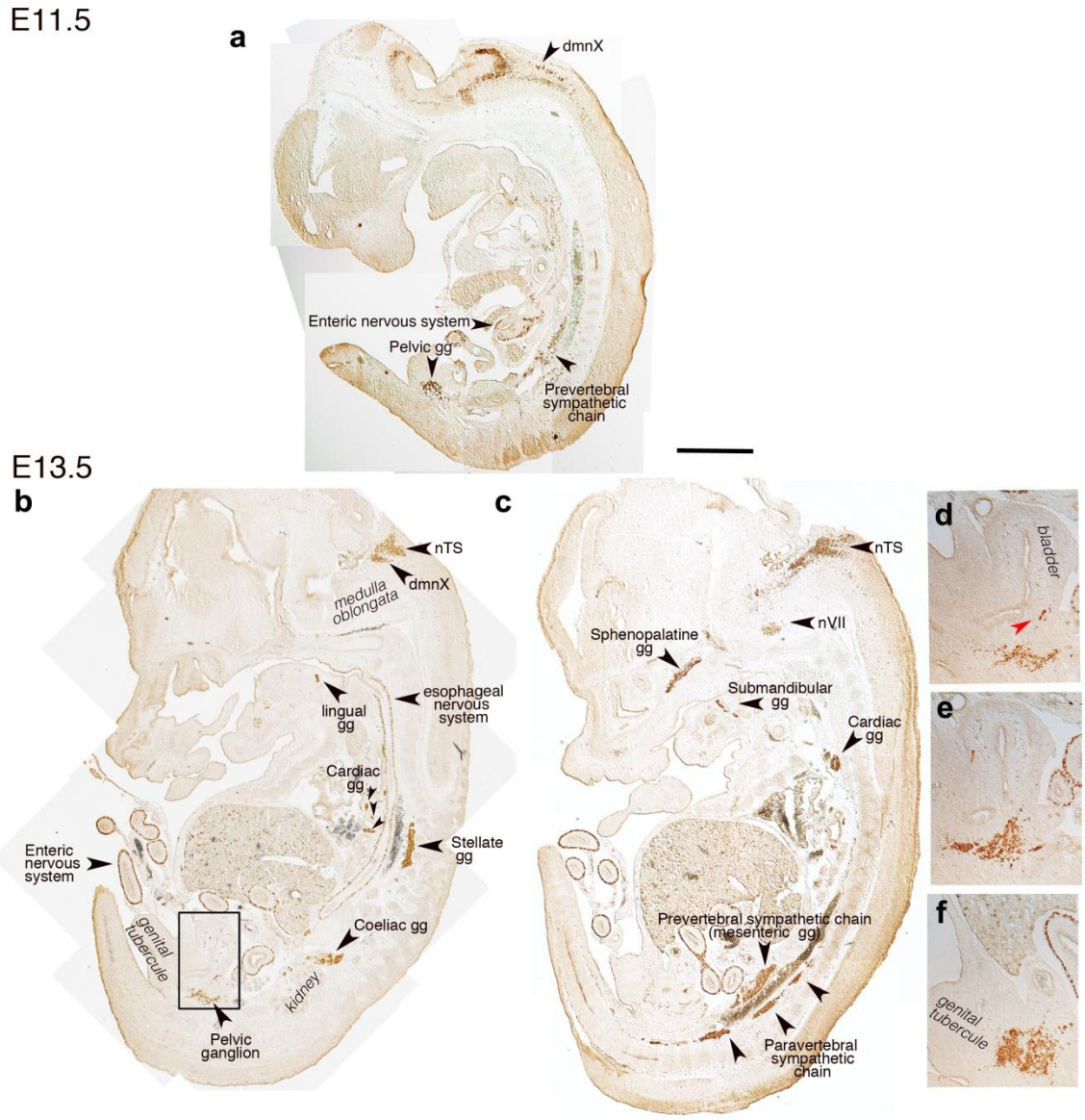

Figure S4

Anatomical location of sympathetic and parasympathetic ganglia in mouse embryos at E11.5 and E13.5. (**a-c**) Parasagittal sections through a whole mouse embryo at E11.5 (**a**) or E13.5 (**b**,**c**), stained by immunohistochemistry for Phox2b. (**d-f**) Parasagittal sections through the urogenital region of an E13.5 embryo, showing different aspects of the pelvic ganglion. (**d**) is a higher magnification of the area boxed in (**b**). Red arrow: an intramural ganglion of the bladder. gg: ganglion; dmnX: dorsal motor nucleus of the vagus nerve; nTS: nucleus of the solitary tract. Scale bar: **a-c**, 1mm; **d-f**, 0.5mm.

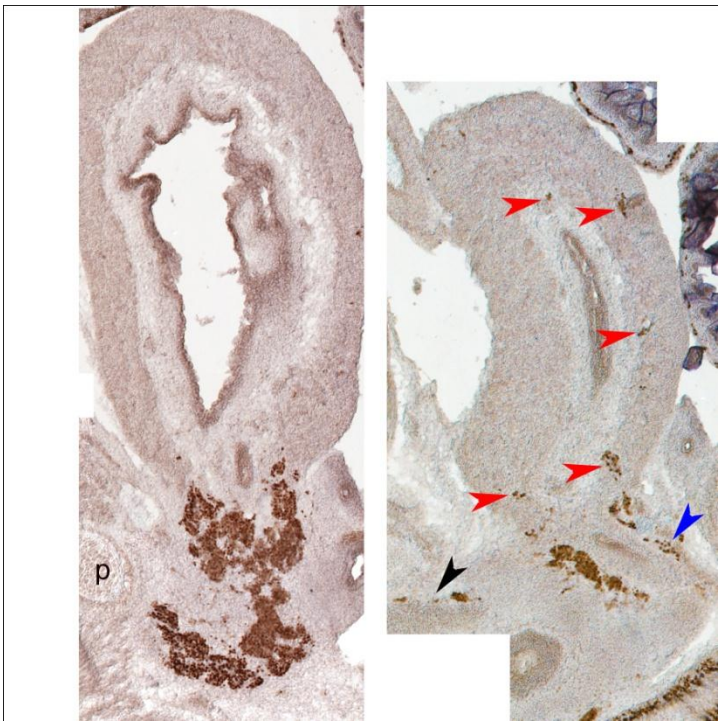

Figure S5

Pelvic and accessory ganglia at E16.5. Two parasagittal sections through the bladder and the pelvic ganglion at E16.5 stained by immunohistochemistry for Phox2b. The main ganglion appears split in a number of lobes. As previously described (*43*), small ganglia or isolated Phox2b+ neurons can be seen in the wall of the bladder (red arrowheads), along the urethra (black arrowhead) and along the ureter (blue arrowhead).

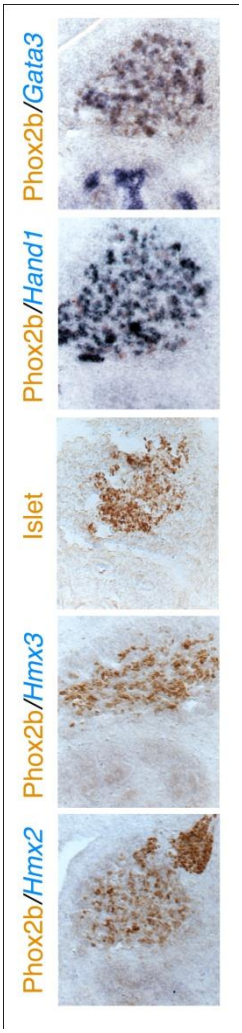

Figure S6

Sympathetic genetic signature of the adrenal medulla. Parasagittal sections through the adrenal medulla at E13.5 stained with the indicated probes or antibodies. The transcriptional signature is Phox2b+/Gata3+/Hand1+/Islet+/Hmx2-/Hmx3-, thus sympathetic.

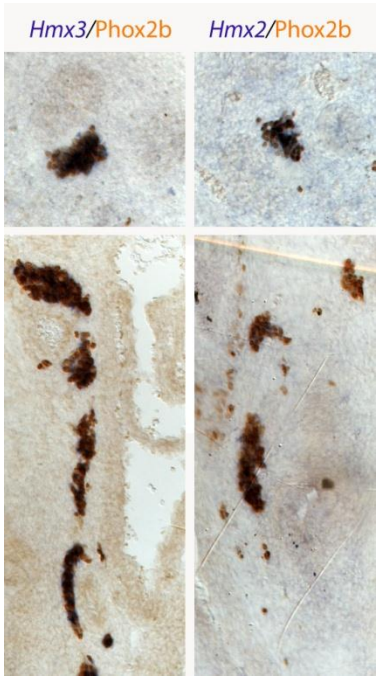

Figure S7

Expression of *Hmx2* and *Hmx3* in cardiac and ciliary ganglia. Parasagittal sections in an E13.5 embryo stained for immunhistochemistry against Phox2b and Hmx3 (left) or Hmx2 (right) in situ hybridization, showing expression of all three genes in the ciliary ganglion (upper panels) and the cardiac ganglia (lower panels).

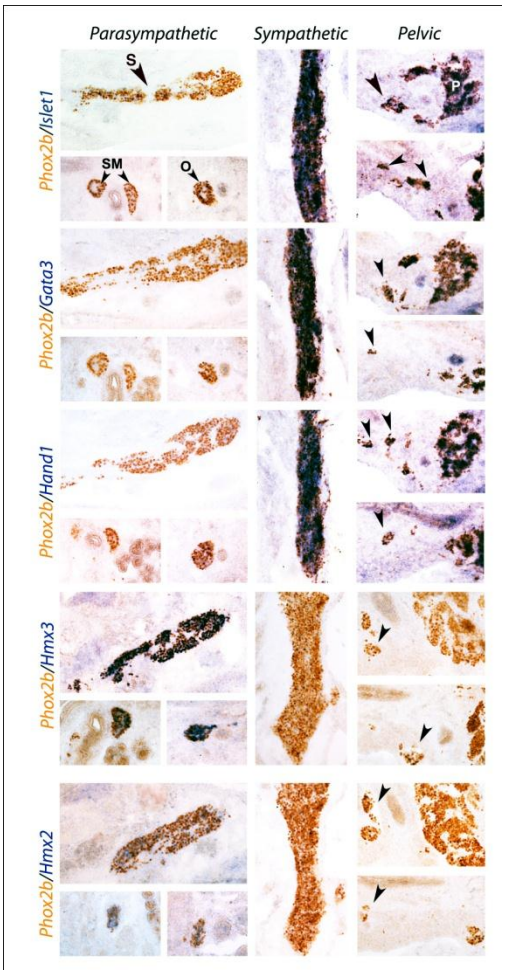

Figure S8

Pelvic and bladder intramural ganglia retain a sympathetic signature at E16.5. Sagittal sections through parasympathetic ganglia (left), the lumbar paravertebral sympathetic chain (middle) and the pelvic ganglion (right) and intramural ganglia of the bladder (arrowheads in the right panels) at E16.5, stained by inmmunohistochemistry for Phox2b, a determinant of all autonomic ganglia (*31*), and in situ hybridization for the indicated probes. O: otic ganglion; S: sphenopalatine ganglion; SM: submandibular ganglion (all parasympathetic ganglia). By this stage *Hmx2* expression has been partially downregulated in parasympathetic ganglia. Note that some intramural ganglia of the bladder have been previously shown to contain noradrenalin (*43*), in line with their sympathetic nature demonstrated here.

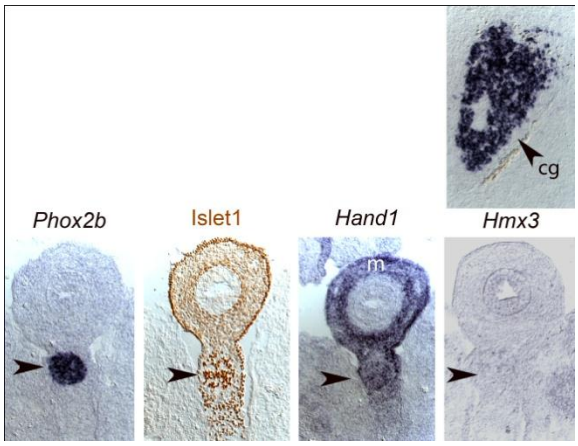

Figure S9

The ganglion of Remak has a sympathetic genetic identity. Transverse sections through a chicken embryo at 5 days post fertilization, passing through the hindgut. The ganglion of Remak (arrowhead) coexpresses Phox2b with the sympathetic markers Islet (detected by an Islet1-2 antibody) and *Hand1*, but not the parasympathetic marker *Hmx3*, which is expressed at the same stage in the ciliary ganglion (cg). Islet and *Hand1* are also expressed in the mesenchymal wall of the gut (m).

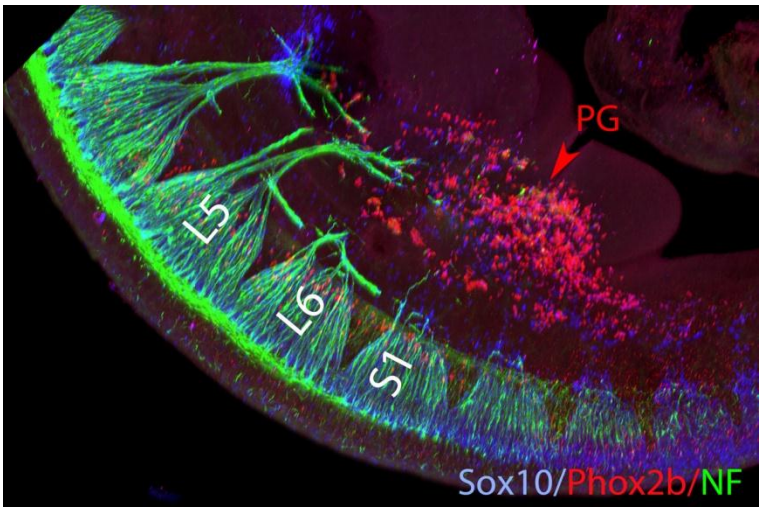

Figure S10

The pelvic ganglion forms in the absence of the pelvic nerve. Wholemount immunofluorescence with the indicated antibodies on an *Olig2*$^{-/-}$ littermate of the E11.5 embryo shown in Fig. 3. In this embryo, no nerve projection is seen at all towards the pelvic ganglion, which nevertheless is present and indistinguishable from its counterpart in heterozygotes (see Fig. 3). L5, L6 and S1: fifth and sixth lumbar and first sacral roots. PG: pelvic ganglion.

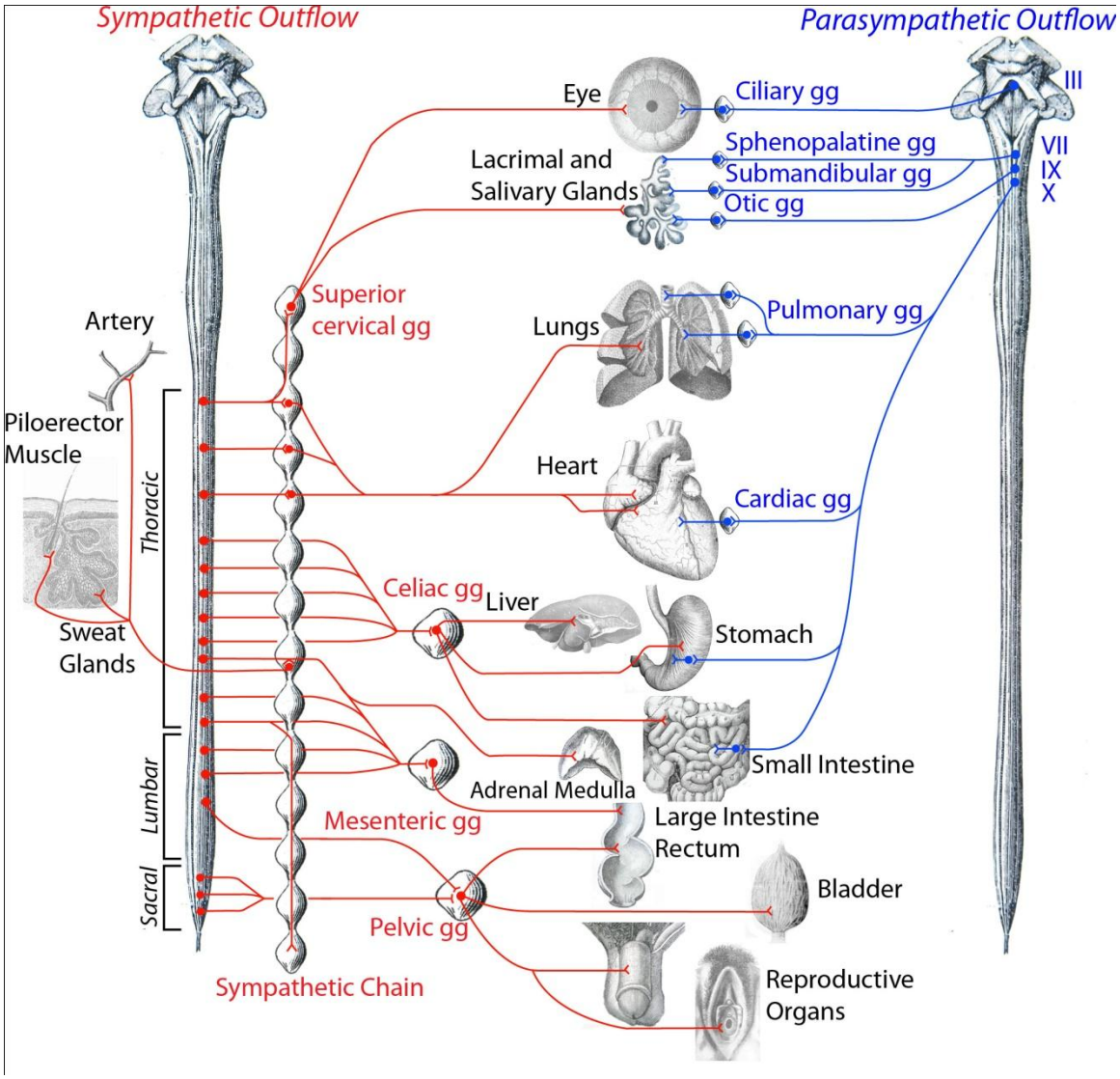

Figure S11. Revised anatomy of the autonomic nervous system. The efferent path of the autonomic nervous system is made up of a spinal sympathetic outflow (in red) and a cranial parasympathetic outflow (in blue). III: occulumotor nerve; VII: facial nerve; IX: glossopharyngeal nerve; X: vagus nerve; gg: ganglion.

Movie S1

The pelvic ganglion at E11.5 in a wild type. The pelvic nerve (in green) reaches the rostral dorsal and lateral edge of the pelvic ganglion (that expresses Phox2b, in red), whose cells lie for the most part distal and medial to them.

Movie S2

The pelvic ganglion at E11.5 in an *Olig2* null mutant. When all motoneurons are deleted, a vestigial pelvic nerve, made up exclusively of sensory fibers, barely touches the pelvic ganglion (that expresses Phox2b, in red), which has the same appearance and size than in wild type embryos (see Movie S1).

References

1. W. H. Gaskell, On the structure, distribution and function of the nerves which innervate the visceral and vascular systems. *J. Physiol.* **7**, 1–80.9 (1886). Medline doi:10.1113/jphysiol.1886.sp000207

2. J. N. Langley, *The Autonomic Nervous System: Part I* (W. Heffer, Cambridge, 1921).

3. E. Kandel, J. Schwartz, T. Jessell, S. Siegelbaum, A. J. Hudspeth, *Principles of Neural Science, Fifth Edition* (McGraw Hill Professional, 2012).

4. J. N. Langley, H. K. Anderson, The innervation of the pelvic and adjoining viscera: Parts II–V. *J. Physiol.* **19**, 71–139 (1895). Medline doi:10.1113/jphysiol.1895.sp000587

5. J. Briscoe, L. Sussel, P. Serup, D. Hartigan-O'Connor, T. M. Jessell, J. L. Rubenstein, J. Ericson, Homeobox gene Nkx2.2 and specification of neuronal identity by graded Sonic hedgehog signalling. *Nature* **398**, 622–627 (1999). Medline doi:10.1038/19315

6. A. Pattyn, M. Hirsch, C. Goridis, J. F. Brunet, Control of hindbrain motor neuron differentiation by the homeobox gene Phox2b. *Development* **127**, 1349–1358 (2000). Medline

7. S. Guthrie, Patterning and axon guidance of cranial motor neurons. *Nat. Rev. Neurosci.* **8**, 859–871 (2007). Medline doi:10.1038/nrn2254

8. A. Prasad, M. Hollyday, Development and migration of avian sympathetic preganglionic neurons. *J. Comp. Neurol.* **307**, 237–258 (1991). Medline doi:10.1002/cne.903070207

9. J. A. Markham, J. E. Vaughn, Migration patterns of sympathetic preganglionic neurons in embryonic rat spinal cord. *J. Neurobiol.* **22**, 811–822 (1991). Medline doi:10.1002/neu.480220803

10. W. A. Alaynick, T. M. Jessell, S. L. Pfaff, SnapShot: Spinal cord development. *Cell* **146**, 178–178.e1 (2011). Medline doi:10.1016/j.cell.2011.06.038

11. P. E. Phelps, R. P. Barber, J. E. Vaughn, Embryonic development of rat sympathetic preganglionic neurons: Possible migratory substrates. *J. Comp. Neurol.* **330**, 1–14 (1993). Medline doi:10.1002/cne.903300102

12. C. R. Anderson, NADPH diaphorase-positive neurons in the rat spinal cord include a subpopulation of autonomic preganglionic neurons. *Neurosci. Lett.* **139**, 280–284 (1992). Medline doi:10.1016/0304-3940(92)90571-N

13. J. S. Dasen, A. De Camilli, B. Wang, P. W. Tucker, T. M. Jessell, Hox repertoires for motor neuron diversity and connectivity gated by a single accessory factor, FoxP1. *Cell* **134**, 304–316 (2008). Medline doi:10.1016/j.cell.2008.06.019

14. J. R. Keast, Plasticity of pelvic autonomic ganglia and urogenital innervation. *Int. Rev. Cytol.* **248**, 141–208 (2006). Medline doi:10.1016/S0074-7696(06)48003-7

15. J. R. Keast, Visualization and immunohistochemical characterization of sympathetic and parasympathetic neurons in the male rat major pelvic ganglion. *Neuroscience* **66**, 655–662 (1995). Medline doi:10.1016/0306-4522(94)00595-V

16. A. Kuntz, R. L. Moseley, An experimental analysis of the pelvic autonomic ganglia in the cat. *J. Comp. Neurol.* **64**, 63–75 (1936). doi:10.1002/cne.900640104

17. W. C. De Groat, A. M. Booth, J. Krier, in *Integrative Functions of the Autonomic Nervous System*, C. M. Brooks, K. Koizumi, A. Sato, Eds. (University of Tokyo Press, Tokyo, 1979), pp. 234–245.

18. U. Ernsberger, H. Rohrer, Development of the cholinergic neurotransmitter phenotype in postganglionic sympathetic neurons. *Cell Tissue Res.* **297**, 339–361 (1999). Medline doi:10.1007/s004410051363

19. K. Huber, P. Narasimhan, S. Shtukmaster, D. Pfeifer, S. M. Evans, Y. Sun, The LIM-Homeodomain transcription factor Islet-1 is required for the development of sympathetic neurons and adrenal chromaffin cells. *Dev. Biol.* **380**, 286–298 (2013). Medline doi:10.1016/j.ydbio.2013.04.027

20. K. Tsarovina, A. Pattyn, J. Stubbusch, F. Müller, J. van der Wees, C. Schneider, J. F. Brunet, H. Rohrer, Essential role of Gata transcription factors in sympathetic neuron development. *Development* **131**, 4775–4786 (2004). Medline doi:10.1242/dev.01370

21. E. Doxakis, L. Howard, H. Rohrer, A. M. Davies, HAND transcription factors are required for neonatal sympathetic neuron survival. *EMBO Rep.* **9**, 1041–1047 (2008). Medline doi:10.1038/embor.2008.161

22. L. Huber, M. Ferdin, J. Holzmann, J. Stubbusch, H. Rohrer, HoxB8 in noradrenergic specification and differentiation of the autonomic nervous system. *Dev. Biol.* **363**, 219–233 (2012). Medline doi:10.1016/j.ydbio.2011.12.026

23. C. L. Yntema, W. S. Hammond, Experiments on the origin and development of the sacral autonomic nerves in the chick embryo. *J. Exp. Zool.* **129**, 375–413 (1955). doi:10.1002/jez.1401290210

24. V. Dyachuk, A. Furlan, M. K. Shahidi, M. Giovenco, N. Kaukua, C. Konstantinidou, V. Pachnis, F. Memic, U. Marklund, T. Müller, C. Birchmeier, K. Fried, P. Ernfors, I. Adameyko, Parasympathetic neurons originate from nerve-associated peripheral glial progenitors. *Science* **345**, 82–87 (2014). Medline doi:10.1126/science.1253281

25. I. Espinosa-Medina, E. Outin, C. A. Picard, Z. Chettouh, S. Dymecki, G. G. Consalez, E. Coppola, J. F. Brunet, Parasympathetic ganglia derive from Schwann cell precursors. *Science* **345**, 87–90 (2014). Medline doi:10.1126/science.1253286

26. S. Nilsson, in *Autonomic Nerve Function in the Vertebrates, Zoophysiology*, vol. 13, D. S. Farner, Ed. (Springer-Verlag, New York, 1983), chap. 2.

27. C. Olsson, B. N. Chen, S. Jones, T. K. Chataway, M. Costa, S. J. Brookes, Comparison of extrinsic efferent innervation of guinea pig distal colon and rectum. *J. Comp. Neurol.* **496**, 787–801 (2006). Medline doi:10.1002/cne.20965

28. K. Fukai, H. Fukuda, Three serial neurones in the innervation of the colon by the sacral parasympathetic nerve of the dog. *J. Physiol.* **362**, 69–78 (1985). Medline doi:10.1113/jphysiol.1985.sp015663

29. W. Jänig, *The Integrative Action of the Autonomic Nervous System: Neurobiology of Homeostatis* (Cambridge Univ. Press, Cambridge, UK, 2006).

30. W. C. de Groat, W. R. Saum, Sympathetic inhibition of the urinary bladder and of pelvic ganglionic transmission in the cat. *J. Physiol.* **220**, 297–314 (1972). Medline doi:10.1113/jphysiol.1972.sp009708

31. A. Pattyn, X. Morin, H. Cremer, C. Goridis, J. F. Brunet, The homeobox gene *Phox2b* is essential for the development of autonomic neural crest derivatives. *Nature* **399**, 366–370 (1999). Medline doi:10.1038/20700

32. E. Coppola, M. Rallu, J. Richard, S. Dufour, D. Riethmacher, F. Guillemot, C. Goridis, J. F. Brunet, Epibranchial ganglia orchestrate the development of the cranial neurogenic crest. *Proc. Natl. Acad. Sci. U.S.A.* **107**, 2066–2071 (2010). Medline doi:10.1073/pnas.0910213107

33. M. R. Elphick, in *Methods in Molecular Biology: Neurotransmitter Methods*, Vol 72, R. C. Rayne, Ed. (Humana Press, 1997), pp. 153–158.

34. A. Ertürk, K. Becker, N. Jährling, C. P. Mauch, C. D. Hojer, J. G. Egen, F. Hellal, F. Bradke, M. Sheng, H. U. Dodt, Three-dimensional imaging of solvent-cleared organs using 3DISCO. *Nat. Protoc.* **7**, 1983–1995 (2012). Medline doi:10.1038/nprot.2012.119

35. A. Pattyn, X. Morin, H. Cremer, C. Goridis, J. F. Brunet, Expression and interactions of the two closely related homeobox genes *Phox2a* and *Phox2b* during neurogenesis. *Development* **124**, 4065–4075 (1997). Medline

36. V. Dubreuil, M. Thoby-Brisson, M. Rallu, K. Persson, A. Pattyn, C. Birchmeier, J. F. Brunet, G. Fortin, C. Goridis, Defective respiratory rhythmogenesis and loss of central chemosensitivity in Phox2b mutants targeting retrotrapezoid nucleus neurons. *J. Neurosci.* **29**, 14836–14846 (2009). Medline doi:10.1523/JNEUROSCI.2623-09.2009

37. M. C. Tiveron, M. R. Hirsch, J. F. Brunet, The expression pattern of the transcription factor Phox2 delineates synaptic pathways of the autonomic nervous system. *J. Neurosci.* **16**, 7649–7660 (1996). Medline

38. H. D. Dufour, Z. Chettouh, C. Deyts, R. de Rosa, C. Goridis, J. S. Joly, J. F. Brunet, Precraniate origin of cranial motoneurons. *Proc. Natl. Acad. Sci. U.S.A.* **103**, 8727–8732 (2006). Medline doi:10.1073/pnas.0600805103

39. F. D'Autréaux, E. Coppola, M.-R. Hirsch, C. Birchmeier, J.-F. Brunet, Homeoprotein Phox2b commands a somatic-to-visceral switch in cranial sensory pathways. *Proc. Natl. Acad. Sci. U.S.A.* **108**, 20018–20023 (2011). Medline doi:10.1073/pnas.1110416108

40. L. Madisen, T. A. Zwingman, S. M. Sunkin, S. W. Oh, H. A. Zariwala, H. Gu, L. L. Ng, R. D. Palmiter, M. J. Hawrylycz, A. R. Jones, E. S. Lein, H. Zeng, A robust and high-throughput Cre reporting and characterization system for the whole mouse brain. *Nat. Neurosci.* **13**, 133–140 (2010). Medline doi:10.1038/nn.2467

41. M. Zawadzka, L. E. Rivers, S. P. Fancy, C. Zhao, R. Tripathi, F. Jamen, K. Young, A. Goncharevich, H. Pohl, M. Rizzi, D. H. Rowitch, N. Kessaris, U. Suter, W. D. Richardson, R. J. Franklin, CNS-resident glial progenitor/stem cells produce Schwann cells as well as oligodendrocytes during repair of CNS demyelination. *Cell Stem Cell* **6**, 578–590 (2010). Medline doi:10.1016/j.stem.2010.04.002

42. C. Sommer, C. Straehle, U. Köthe, F. A. Hamprecht, ilastik: Interactive learning and segmentation toolkit. 2011 8th IEEE International Symposium on Biomedical Imaging (ISBI 2011) 230–233 (2011). doi:10.1109/ISBI.2011.5872394

43. A. El-Badawi, E. A. Schenk, The peripheral adrenergic innervation apparatus. I. Intraganglionic and extraganglionic adrenergic ganglion cells. *Z. Zellforsch. Mikrosk. Anat.* **87**, 218–225 (1968). Medline doi:10.1007/BF00319721